CHAPTER 2

Hydroelectric Power Generation Systems and Experimental Rig

2.1 Introduction

This chapter presents the hydroelectric power generation systems and the experimental setup of the doubly-fed induction generator using a back-to-back three-level neutral point clamped (NPC) voltage source converter (VSC) which is used to experimentally examine the direct power control techniques. This experimental system is comprised of the hardware development in the setup. A main power circuit for the three-level NPC VSC, the dc-link capacitor in a back-to-back converter, grid filter, the interfering to gate driver circuit, gate driver circuit, and measurement circuits of voltage and current are designed and built.

2.2 Hydroelectric power generation

The large scale hydroelectric power generation uses the large reservoirs of earth surface water, which create by the dam and the reservoir to retain water from a river. The water is allowed to flow out of the reservoir in a controlled manner and rotate turbines, which drives electrical generators to produce electricity. The potential difference forces water to flow through a turbine, which transforms the potential energy into mechanical energy. The turbine drives an electrical generator which converts the mechanical power into electrical energy.

In recent year, many small sizes of small-hydro power plants are developed, because it has very good performance and feasible with cost effective, reliable energy technology to be considered for providing clean electrical generation, and high efficiency. The small-hydro plant is generally defined as electricity generation capacity about 50-200 kW. Many of these systems are run-of-rivers. These small hydro power plants meet the

purpose in the remote areas. The critical problem of small hydro power plants is maintenance for a difficulty in local.

There are several advantages of hydroelectric power plants [1], [27], [28]:

- Hydroelectric power plant projects provide multidiscipline developments for the target are such as flood control, irrigation and water supply.
- High efficiency of power conversion and a high capacity factor, compared with 10% for solar energy and 30% for wind energy.
- Slow rate of change, the output power varies only gradually from day to day, not from minute to minute.
- No greenhouse gas emission and no fuel required to generate electricity.
- Hydro generators are effective in providing critical services to maintain reliable operation of power systems.

A water flow from an upper to a lower level represents a hydraulic power potential. The potential energy of water PE from the upper to the lower level is given by [29]

$$PE = gH_A, \tag{2.1}$$

where PE is the potential energy (J), g is the acceleration of gravity (9.81m/s^2), and H_A is the available head (m).

The available power from the hydro can be expressed as,

$$P_A = \eta_g \eta_t \rho g Q H_A, \tag{2.2}$$

where P_A is the available power of the hydro (W), η_g the efficiency of the generator, η_t the efficiency of turbine, ρ the density of the water (kg/m^3), Q the flow rate of the water (m^3/s).

In real hydro systems, the water delivered to the turbines will lose some energy as a result of frictional drag and turbulence as it flows in channels and pipes. Therefore, the effective head H_E will be less than available head $\left(H_E < H_A\right)$. In addition, the efficiency of turbines varies according to the type of turbine and the flow rate into

turbine. The system efficiency considers both the combined efficiency of the generator $\left(\eta = \eta_g \eta_t\right)$, converting mechanical to electrical energy, and the turbine. Therefore, the electric power of the hydraulic power P_{hydro} can be calculated as [2],

$$P_{hydro} = \eta \rho g Q H_E. \tag{2.3}$$

The potential energy in water is converted into mechanical energy in the small turbine as results of the water pressure which applies a force on the runner blades and then decreases as it passes through the reaction turbine. The relation between the mechanical hydraulic power $P_{m,hydro}$ and the hydraulic power P_{hydro} can be obtained by using the hydraulic turbine efficiency η_{hydro}, as expressed [28]:

$$P_{m,hydro} = \eta_{hydro} P_{hydro}. \tag{2.3}$$

2.3 Overall structure of the prototype system

The basic structure of the experimental setup is shown in Figure 2.1. The experimental setup is consisting of a 1 kW, 380 V, 50Hz, and 4-pole DFIG generator mechanically connected to a prime mover, which operated torque producing motor. The stator of DFIG is directly connected to the utility grid, while the rotor is fed by the back-to-back three-level NPC VSC. The back-to-back convertor consists of two converters (rotor-side converter and grid-side converter) that are "back-to-back" connected. Between the two converters a dc-link capacitor is placed, as energy storage. The converter uses 1200V insulated-gate bipolar transistor (IGBT) power switches with a dc-link voltage of 180V. A 9.42 kW 4500 rpm permanent magnet synchronous machine (PMSM) is used to emulate a hydro turbine. The PMSM is driven by a four quadrant made by Siemens.

The experimental system is controlled by a DS1103 PPC controller board produced by dSPACE. The software in experimental system is easy to learn and is extremely flexible which leads to fast development time. The controller can be accessed from the host computer through graphically oriented tools for on-line visualization and on-line parameter tuning, which carry out the various control functions, data acquisition, PWM

generation and data communication with the host computer. Control desk combines the cockpit and trace options together in the same window. The most significant advantage in using the DS1103 is the relative ease of use, freeing the designer from the burden of manually programming the Digital Signal Processing (DSP). A total of 9 Hall-effect current measurements and 7 voltage measurements are employed, and encoder is used to provide a measurement of speed.

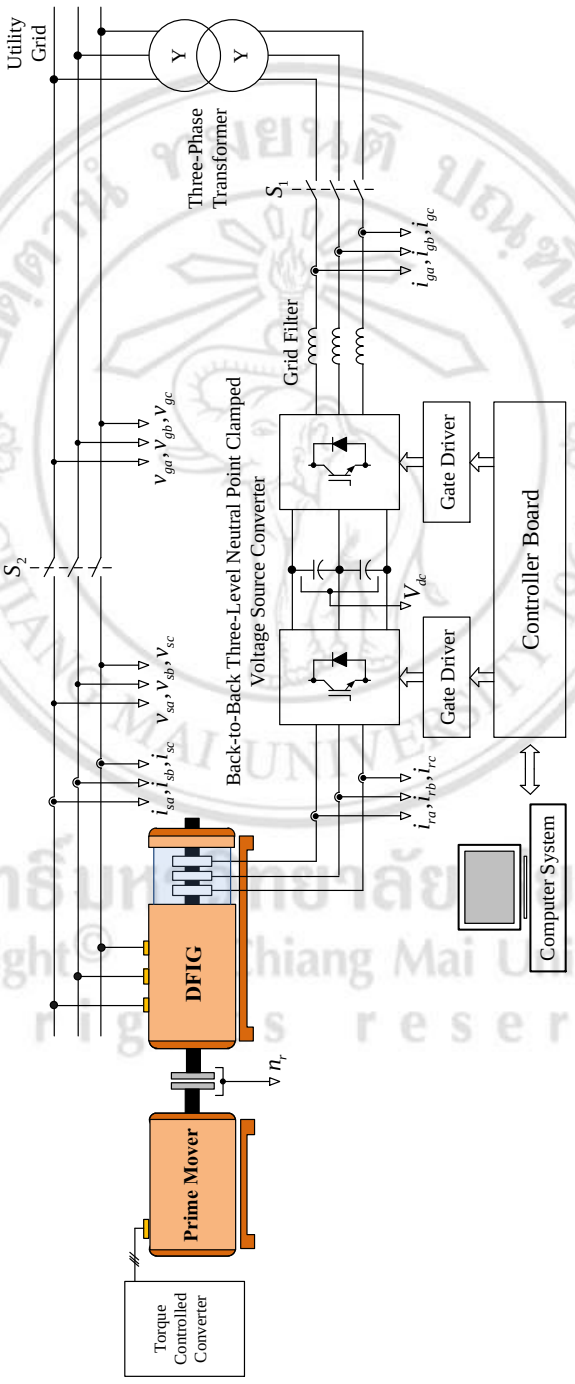

Figure 2.1 The overall structure of the experimental setup.

2.4 Generator and prime mover

The main component in the setup is a 1kW DFIG produced by Lucas Nulle. The generator is connected with a wye-connected stator and delta-connected rotor. The prime mover motor or torque producing motor is a 9.42 kW permanent magnet synchronous motor (PMSM) made by Siemens. The prime mover motor is fed by a torque controlled converter, SIMOVERT MASTERDRIVES.

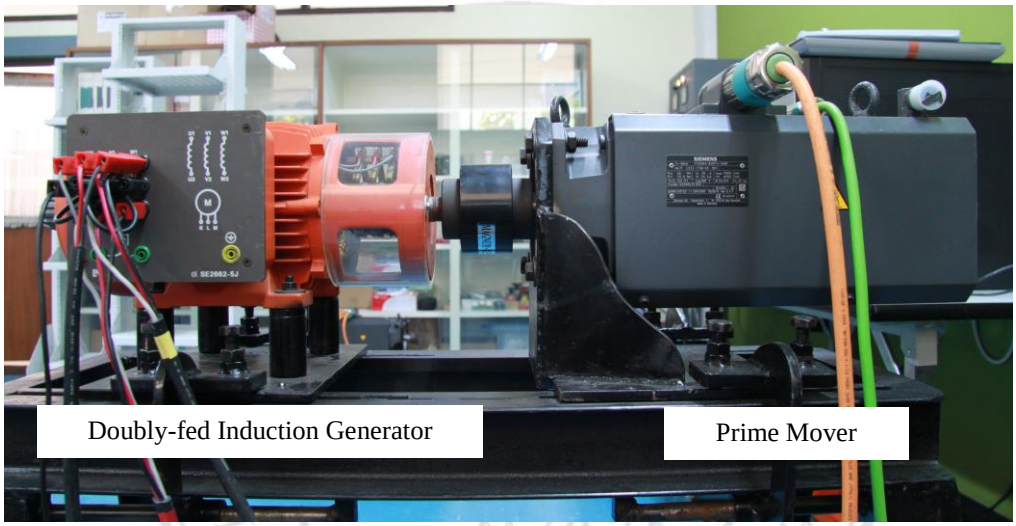

Figure 2.2 Experimental setup with prime mover and DFIG.

Figure 2.2 shows the prime mover and the generator for this thesis. The generator used in the experimental setup is a wound rotor induction machine. The characteristics and parameters of the generator used in this thesis are shown in Table 2.1:

Table 2.1 Doubly fed induction generator specification

Nominal values of the DFIG:		
Rated power	1	kW
Rated stator voltage (wye-connected)	380	V
Rated rotor voltage (delta-connected)	127	V
Rated stator current	2.9	A
Rated rotor current	4.9	A
Rated stator frequency	50	Hz
Nominal rotor speed range	1200-1800	rpm
Number of pole pairs	2	
Stator-rotor turn ratio	1.732	
DFIG parameters:		
Stator resistance	7.9	Ω
Rotor resistance	8.8	Ω
Stator leakage inductance	78	mH
Rotor leakage inductance	78	mH
Magnetizing inductance	700	mH

2.5 Power converter and passive components

2.5.1 Power converter

A photograph of the implemented back-to-back three-level NPC VSC as is shown in Figure 2.3. The IGBT modules are Semikron's SKM50GB123D. It is a 1200V IGBT with an integrated anti-parallel fast diode module. The clamp diodes are Semikron's SKKD42F12, a 1200V fast diode module. Each single phase of three-level NPC VSC is implemented, equipped with the two switch IGBT modules and the single clamp diode module. The switch modules of the converter are constructed on a shared the air duct by the heat sinks.

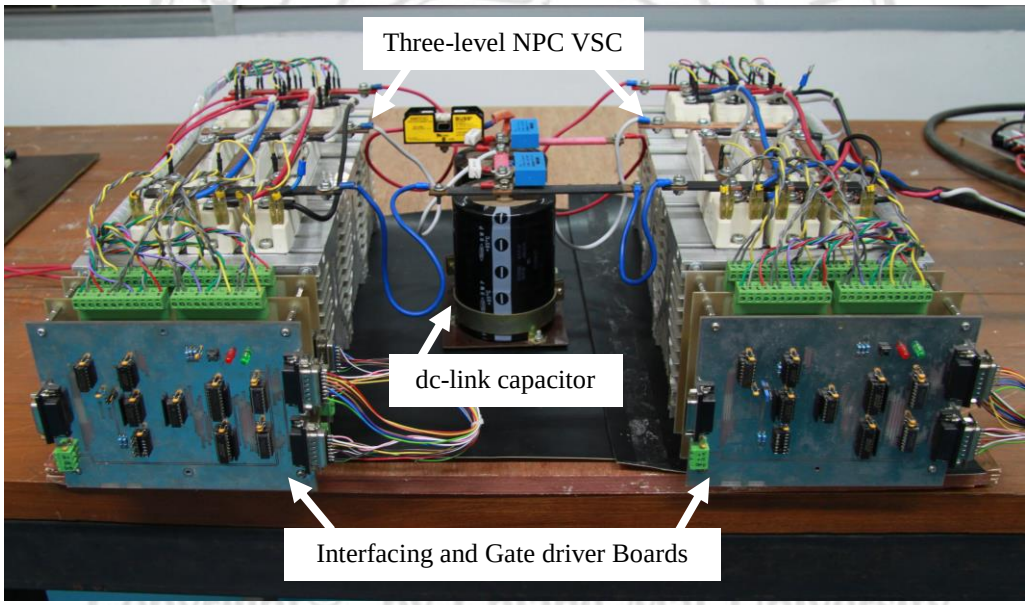

Figure 2.3 The back-to-back three-level NPC VSC.

2.5.2 dc-link capacitor

The dc-link capacitor serves as energy storage. The current in the dc-link can be derived from the ac power at either side, since the dc power must equal the power on the ac side when neglecting the losses. The large capacitor size of the dc-link is selected. Because the large capacitor has a slow response to the voltage changes, the current in each capacitor can is smaller, therefore increasing its lifetime. The dc-link capacitor used in this

thesis consists of two 4700 μF, 450 V electrolytic capacitors, which is made with a series connection as shown in Figure 2.3. This gives a 2350 μF, 900 V. When capacitors are series connected it is normal to reduce the voltage level due to asymmetry in the capacitors. Reducing is not necessary with this dc-link since the neutral point is measured, and kept balanced. The initial charging current into the filter capacitor is limited by the resistor which is short circuited by a contactor as the dc-link builds up to 85% of its nominal voltage.

2.5.3 Grid filter design

The grid filter reduces the current harmonics infected to the utility grid. The design of this device considering the voltage drop in the inductor, analyzing the current ripple in high switching frequency, and identifying the harmonic spectrum generated by the grid-side converter. The size of the three-phase grid filters are 12 mH, which are chosen for three-level NPC VSC.

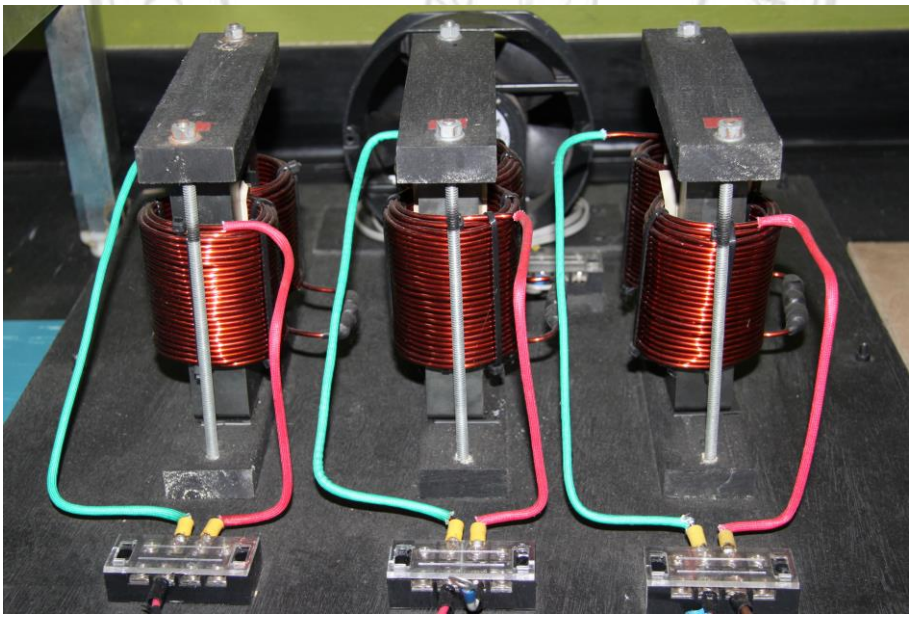

Figure 2.4 The grid filters.

2.6 Controller board

The control system for back-to-back three-level NPC VSC has been implemented in the DS1103 PPC controller board produced by dSPACE. It is a mixed RISC/DSP digital controller providing a powerful processor for floating point processor calculations. The DS1103 PPC card is plugged in one of the ISA slots of the mother-board of the host computer, as shown in Figure 2.5. The control system has been developed using Matlab/Simulink and then automatically processed and run in the DS1103 PPC card. A Graphical User Interface (GUI) has been built using the software Control Desk of dSPACE. It allows the real-time evaluation of the control system.

Figure 2.5 The DS1103 PPC controller board.

The block diagram of the DS1103 is shown in Figure 2.6. The signal groups used in the experimental set-up are I/O interfaces, A/D channels, D/A channels.

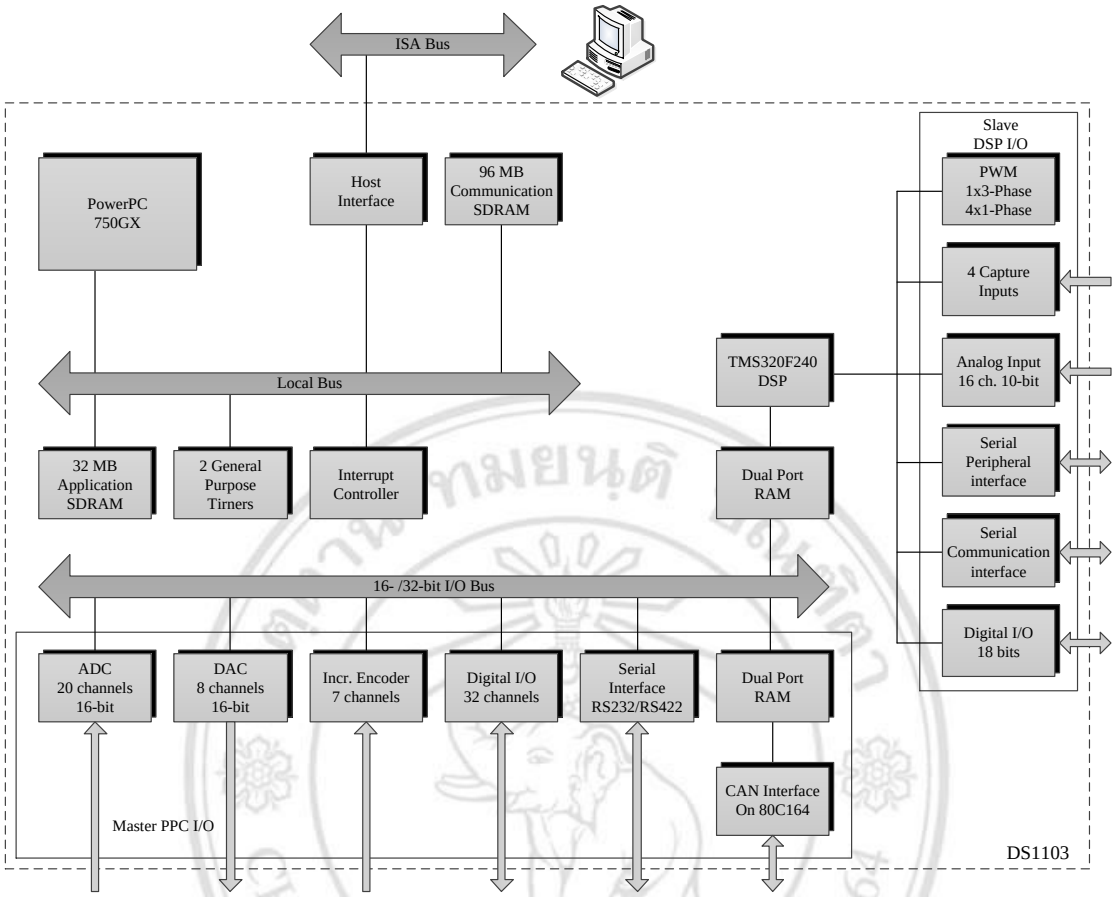

Figure 2.6 Block diagram of the DS1103 PPC controller board.

2.7 Interface boards

The interface board for back-to-back three-level NPC VSC fed DFIG system is accomplished by the interfacing to gate driver circuit, gate driver circuit, voltage measurement circuit and current measurement circuit. The details of each circuit are described in following subsections.

2.7.1 Interfacing to gate driver

The control interface permits the transfer of the PWM switching signals generated in the dSPACE controller board to the gate drivers (SKHI 61), providing electric isolation. This interface board protects the system against short circuit and power supply low voltage condition, which is performed by interpreting the error signals of the gate drivers (Error 1 and Error 2). Moreover, the control interface is able to interrupt the operation, by

software program, if conditions of over voltage and over current are detected in the power circuit (Error 3 and Error 4). Figure 2.7 shows the implemented electrical diagram for the interface to gate driver circuit. The buffer (74LS20 and 74HC73) supports the PWM switching signals coming from the dSPACE controller board. The buffer stops the PWM input signals if any error condition is detected. The level shifter for TTL to CMOS (MC14504B) is a hex non-inverting level shifter using CMOS technology for the PWM switching signals produced in dSPACE controller board.

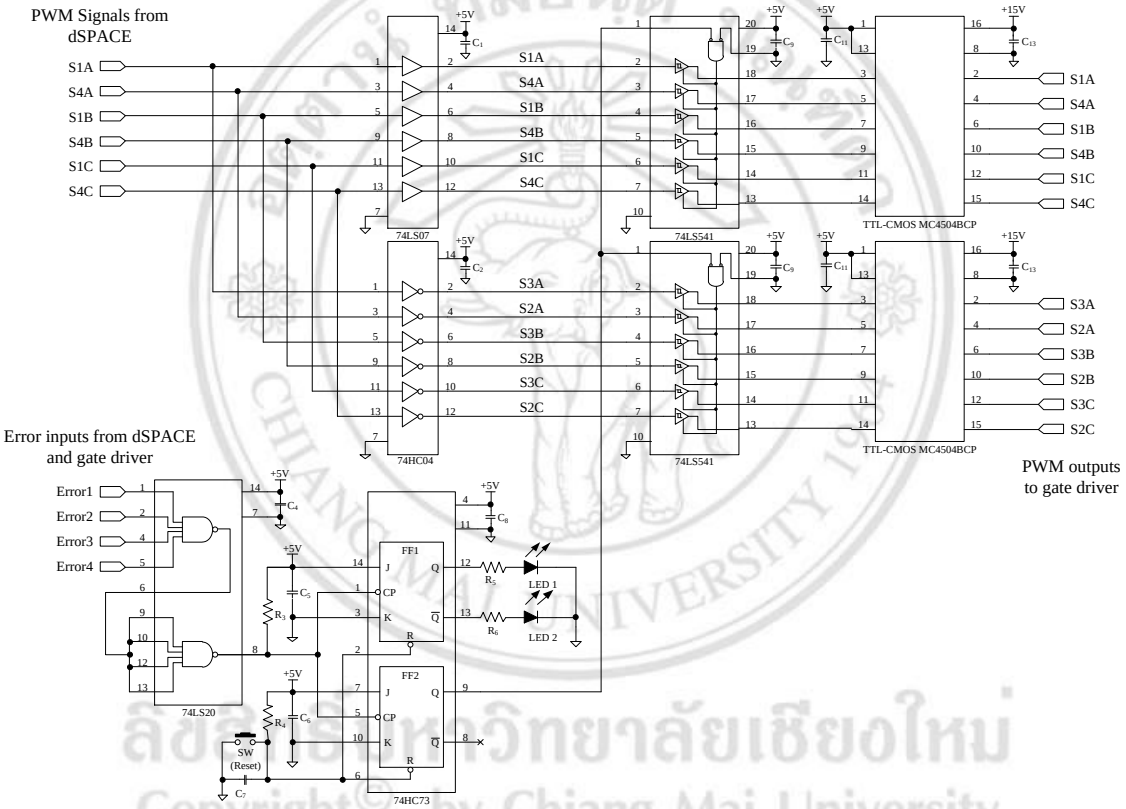

Figure 2.7 The interfering to gate driver circuit.

2.7.2 Gate driver circuit

The control signals to the IGBT power switch is usually supplied by a logic circuit consisting of some dedicated controller. The signal output stage of such logic circuits cannot drive the IGBT gate directly because it is often not designed to provide gate current and voltage with appropriate

magnitude in both the positive and negative direction. Therefore, it needs a gate drive circuit to interface the logic control signal to gate of the IGBT.

In this thesis, the three-level NPC VSC has twelve IGBT power switches. Therefore, a normal three phase gate driver module for a standard two-level converter is not sufficient. Each converter is equipped with two six-pack driver circuits from Semikron SKHI 61. Figure 2.8 shows the implemented electrical diagram of gate driver circuit for three-level NPC VSC. This driver takes care of interlocking and dead time. Under normal operation, the SKHI 61 has an interlocking function, which sets the dead time to prevent both the top and the bottom IGBT from being switched on simultaneously. Moreover, the gate driver has built-in protection and status indication circuits for over-current, short circuit, and under-voltage.

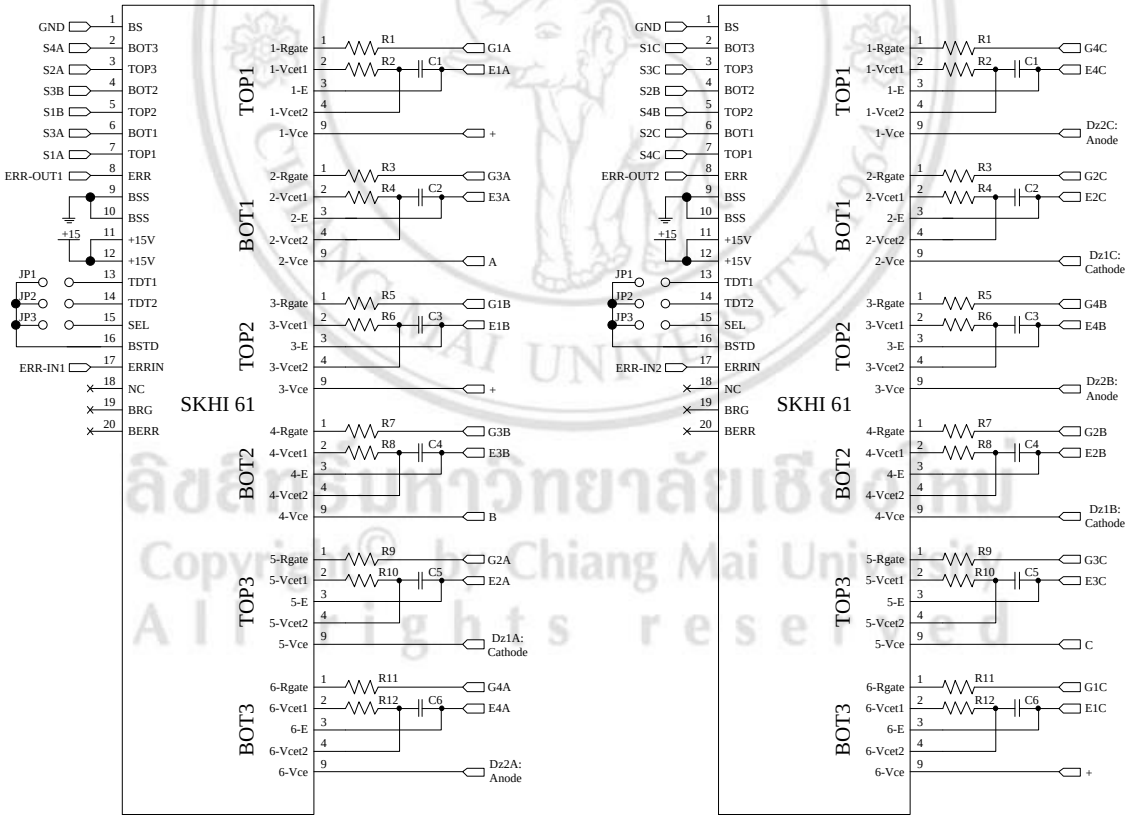

Figure 2.8 Gate driver circuit for three-level NPC VSC.

2.7.3 Voltage and current measurement

As shown in Figure 2.9, the measurement circuits consist of voltage and current sensors. The principles of voltage and current measurements are the same. The sensors for voltage and current are isolated from the power circuit and a separate power supplies are used to avoid any effect on the voltages and currents being measured.

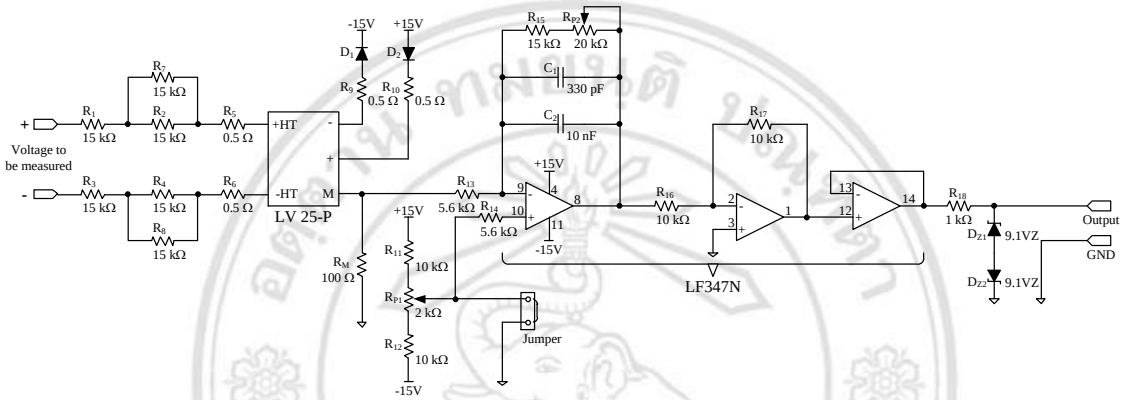

(a)

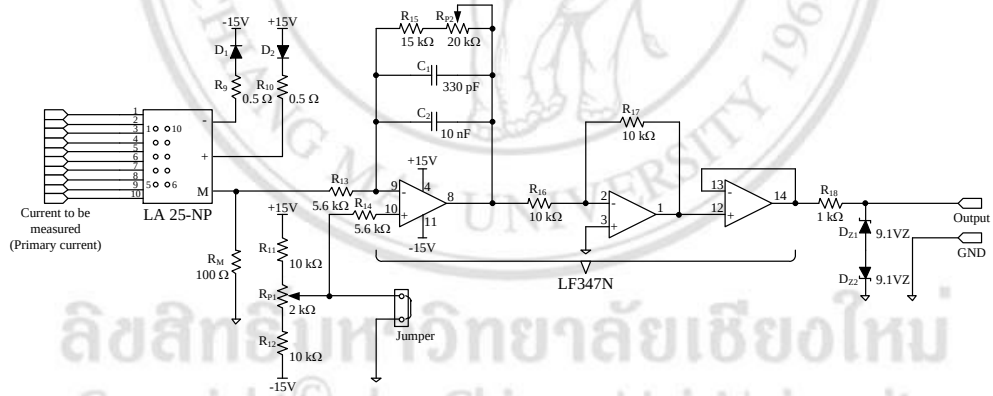

(b)

Figure 2.9 The schematic diagram of voltage and current measurement systems (a) Voltage measurement circuit (b) Current measurement circuit.

For voltage measurement, the schematic diagram of the voltage measurement circuit is shown in Figure 2.9 (a). To measure the voltages, LV 25-P, are used, which produced by LEM components. It is the transducer used for the electronic measurement of dc and ac voltages. The sensor circuit is designed in such a way that it will be able to measure the

full range of the applied voltage. The nominal primary voltage is set as 230 V for ac voltage and 750 V for dc-link voltage. A primary resistor, R_1-R_8, is used to generate a primary current linearly proportional to the measured voltage. This current produces a magnetic flux, which in turn is proportional to the voltage. The magnetic flux is constantly controlled at zero by a compensating current flowing through the secondary coil using the Hall-Effect device and associated electronic circuit, which generated a secondary current with the conversion ratio of 2500:1000. The secondary current multiplied by measurement resistor R_M is used to generate the output voltage of the sensor. The signal conditioning part of the circuit is calibrated by adjusting the potentiometer R_{P2} in such a way that the maximum voltage to be measured gives an output voltage signal of peak value $\pm 10\,\mathrm{V}$. To protect the ADC input of the controller board from over voltage, two zener diodes, with breakdown voltage of 9.1 V, are connected back to back for limiting signal circuit.

The current transducer used in the current sensor circuit is an LA 25-NP produced by LEM Components. The connection of the current transducer is shown in Figure 2.9 (b). Similarly to the voltage transducer, the current transducer uses the Hall-Effect to measure ac current, generating the secondary current with the conversion ratio 5:1000 to the primary current. The secondary current multiplied by measurement resistor R_M is used to generate the output voltage of the current sensor. The signal conditioning part of the circuit is calibrated by adjusting the potentiometer R_{P2} in such a way that the maximum voltage to be measured gives an output voltage signal with peak value of $\pm 10\,\mathrm{V}$. To protect the ADC input of the controller board from over voltage, two zener diodes, with breakdown voltage of 9.1 V, are connected back to back for limiting signal circuit, which are similar to that of the voltage measurement set-up.

2.8 Conclusion

In this chapter, an explanation of the hydroelectric power generation system, generator system and the hardware implementation of the three-level NPC VSC topologies have been presented in this chapter. The design of each circuit for the prototypes consists of the power converter, dc-link capacitor, the grid filter, the interfering to gate driver, the gate driver circuit, voltage and current measurement circuit, and the control platform. The explanation of the functionality and construction of these components has been described.